

ACCURATE TB MANIFESTATION USING MULTI CLASS SVM CLASSIFIER

Mr.P. JohnVivek¹, Swathika.S.R²

¹Asst.Professor, Department of ECE, Paavai Engineering College, Namakkal, India.
E-mail: Vivekselvampec@paavai.edu.in

²Department of ECE, Paavai Engineering College, Namakkal, India
E-mail: jsswa2015@gmail.com

Abstract

TB is one of the leading cause of death worldwide, with a mortality rate of over 1.2 million people in [2010].When TB is left undiagnosed, mortality rates will be high. This paper presents an accurate approach for detecting TB using a well-known classifier known as the Multiclass SVM classifier. In this paper, we first extract the lung region using a graph cut segmentation method. For this lung region, we compute a set of texture and shape features, which enables the X-rays to be classify the lung region as normal, moderate or severe(TB affected) using a Multi-class SVM Classifier. In an effort to reduce the burden of TB, this recent approach achieves a maximum accuracy in identifying TB. This proposed system for TB manifestation achieves an accuracy of 94.3% compared with the earlier methods [1] which achieves an accuracy of 86%.We collect the dataset from SKS hospital and perform the classification for the received dataset. We compare the performance of the received dataset with the classifiers: KNN, SVM & Multi-class SVM classifier. Among the classifiers, the Multiclass SVM Classifier achieves a maximum accuracy. Hence the Multi-class SVM classifier is promising in achieving the maximum performance up to the human experts.

Index Terms: CAD and diagnosis, lung nodule, pattern recognition and classification, segmentation, tuberculosis (TB), X-ray imaging. Multiclass SVM classifier.

1. INTRODUCTION

TUBERCULOSIS (TB) is a major health problem worldwide, with a mortality rate of over nine million people every year. TB is caused by infectious bacteria known as the Mycobacteria tuberculosis, which typically affects the lungs. It is one of the communicable disease which transfers through air by coughing and sneezing. TB is caused mainly due to the lack of immunity as well as malnutrition. TB has further created an urgent need for a cost effective screening technology to monitor progress during treatment.

There are several antibiotics which are effective in treating TB. But the drawback is that, identifying TB is difficult and hence this the main cause for mortality worldwide. Tuberculosis is identified by collecting the pus samples of TB patients, but there is a disadvantage, because it is difficult to identify the growth of the mycobacterium as it is a slowly growing

organism. Hence, diagnosing TB is a great challenge.

In this paper, we have presented an accurate approach for detecting TB in CXRs using lung segmentation and classification using the Multi-class SVM classifier. Identifying TB from CXRs is also a challenge, because the CXR sometimes correlates with the chest x-rays obtained from HIV patients. Hence proper health education should be provided about HIV and TB. Intake of wrong drugs must also be avoided by creating an awareness among the people. Over the past few century, people doesn't have enough education about the communicable diseases. But there is a urgent need today for the survival of every living beings, because the life expectancy has been decreased by various deadly diseases. Achieving a maximum life span nowadays is a difficult thing, because of this communicable diseases. Hence this accurate method is implemented for diagnosing TB with low cost, for the survival and increase in life span of the poor and middle class people.

Some of the latest development for detection of TB are molecular diagnostic tests that are fast, accurate, highly sensitive and specific. However, financial support is required for these tests.



Fig.1 Example of normal CXRs.

In this paper, we present an accurate approach for detecting TB manifestations in chest X-rays (CXRs), based on our earlier work in lung segmentation and lung disease classification. An accurate approach to X-ray reading allows mass screening of large populations that could not be managed manually. A poster anterior radiograph (X-ray) of a patient's chest is a mandatory part of every evaluation for TB. The chest radiographs obtained must be collected from the specific hospital for an effective diagnosis of TB. Some of the works included are associated with our previous papers, such as the image processing techniques. CAD assists a strong place in analyzing lung cancer and detection of cancer nodules but it

is not effective in identifying TB.

Our proposed work is cost based; which finds a major place in increasing the life expectancy of poor and middle class people. The classifier used here is a best classifier in achieving accuracy and hence finds a major place in diagnosing TB in future. The comparison graph provided in this method explains the effectiveness of the classifier in its accuracy. Some of the classifier provided in our earlier works has a maximum disadvantage but there is no need to worry about the Multi-class classifier which is very effective in classifying the stages of TB as: normal, moderate and severe. The data sets we have collected are from a standard hospital and it contains many individual CXRs. We would have a belief that this method achieves a maximum expectancy of the human experts, as this method concerns with low cost. The main aim of this classifier is the classification of the lungs with three main stages namely: normal, moderate and severe. As drug intake causes side effects and critical problems in future, we must identify TB in its early stage as "PREVENTION IS BETTER THAN CURE".

Fig.1 shows examples of normal CXRs without signs of TB. These examples are from SKS dataset that we describe in more detail in Section III. Fig. 3 shows positive examples with manifestations of TB, which are from the different dataset. Typical manifestations of TB in chest X-rays includes infiltrations, cavitation's, effusions and military patterns. For instance, CXR in Fig. 3 have infiltrates in both lung cavities.

In this paper, we describe how we discriminate between normal and abnormal CXRs with manifestations of TB, using image processing techniques. We structure the paper as follows. Section II discusses related work and shows the state of the art. Section III briefly describes the datasets we use for our experiments. In Section IV, we present our approach with lung segmentation, feature computation, and classification. A pre-sensation of our practical experiments follows in Section V. Finally, a brief summary with the main results concludes the paper. Note that some of the features we use in this paper are identical to the features used in one of our earlier publications. However, the lung boundary detection algorithm in this paper differs from the one used in our earlier publication.

2. RELATED WORK

In the earlier technique [1], SRI tree stereo pair finds a major place in assigning a label (such as a disparity) to every pixel. A common constraint is that the labels should vary smoothly almost everywhere while preserving sharp discontinuities that may exist, eg.at object boundaries. Here, we consider a wide class of energies with various smoothness constraints. The results of minimizing with the Potts converges the running time from 79sec to 94sec, respectively. This is not

up to the global optimum. Hence there should be an improved performance and hence this technique finds a drawback. Now proceeding to the next literature [2] the technique used is the K-NN (K Nearest Neighbours). This paper describes the main problem in the texture analysis of chest radiographs in the complex back round of super; imposed normal anatomical structures to which the analysis must be a one-how insensitive. One way to solve this problem would be to resist the texture analysis to ROIs that do not contain normal structures such as (crossing0rib borders and large vessel projections. The KNN is a non-parametric method used for classification and regression. In this case, the input consists of the K-closest training examples in feature space. In KNN classification, the output is a class membership. An object is classified by a majority vote of its neighbours. If K=1, then the object is simply assigned to the class of that simple nearest neighbour. In KNN regression, the output is the property value of the object. This value is the average of the values of its K nearest neighbours. The technique finds a drawback eventhough it yields a good ID database. The results are from 0.986-0.0062. For different scales. The drawback is that it is not applicable to all cases of abnormal findings in TB screening. Technique [3] uses field extraction from x-ray such as heart, clavicles and ribs based on an adaptive segmentation method. It can increase the accuracy about 80.75% but this is not up to the human experts and hence this method finds a drawback. Technique [4] uses a edge-based Gradient Magnitude freatures. Accurate measurement of all cell cycle progression is useful for understanding disease process such as cancer and high-throughput anti-cancer drug screening studies. The edge-based Magnitude Histogram, we use 30 edge orientation Histogram descriptor. The technique finds many useful applications among the people. It enables quantitative studies of cellular process in high-throughput studies involving large test series. The result is that PCNA assumes different patterns of throughput in the cell cycle phases. The results may vary greatly from a low of 30% (A2, PCNA) to a high of 73% (EV, PCNA). But the drawback is that, A1 feature for and EV feature for the second channel perform poorly such as the gradient magnitude and A2 feature for the second channel. In technique [5] we use the Gaussian filters, Hessian matrix and Binary classifier. Eventhough several skin tests are available based on whether the individual has been exposed to TB, our processing steps includes lung field extraction in the x-rays. It finds an accuracy of about82.4% and finds a drawback because we implement a technique in future with more accuracy. In technique [6] with the feature extracted from the average lung model. The graph cut algorithm models computer vision labeling problems such as energy minimization using an undirected weighted graph $G=(V,E)$.The result is that each marker in the graph represents the dsc score of an x-ray image in the set. For eg.dsc=0.80.The average dsc of the set is 0.97-0.037.The major disadvantage in this technique is that there are different segmentation problems, such as low illumination, array of signs, similar back round colour and occlusions. In the technique [7] we use ASM/HDAP algorithm. Obtaining an accurate segmentation of the clavicle is used for a wide range

of applications. The addition of other algorithms significantly improves segmentation performance compared to the previous state of the art algorithm. The result is that the performance of HDAP is increased and finds an accuracy of 86.5%. The drawback is that ASM mechanism generates plausible shapes and also limits how accurate it can outline the borders of a previously unseen instance of the structure. The technique [8] uses the log gabor mark algorithm. The journal was published in the springer-verlag Berlin Heidelberg in 2010. The radiographs are an important part of any medical evaluation for TB, among many microbiological smears, cultures, and skin tests. A reliable screening system for TB detection on radiographs is therefore a big step towards more powerful TB detection on radiographs is therefore a big step. TB related abnormalities in chest x-rays are diffuse, and discriminating between normal anatomical structures and abnormal patterns. Gabor filters used here are a traditional choice for obtaining localized frequency information.

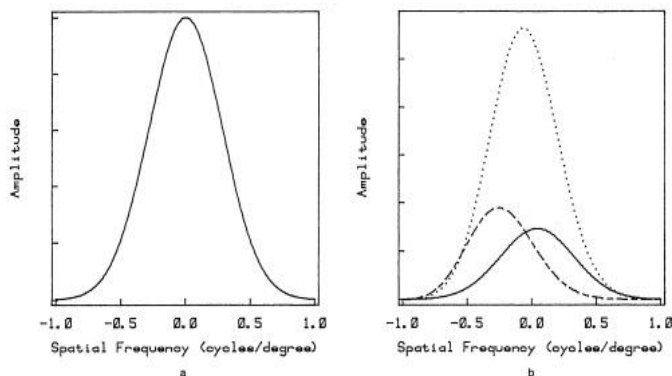


Fig.2 Log Gabor Transfer Function[Tech2:ex]

However there are two limitations. The maximum bandwidth of a gabor filter is limited to approximately one octave and Gabor filters are not optimal if one is seeking broad spectral information with maximal spatial localization.

$$G(W) = e^{-\log(w/w_0)^2} / 2(\log(k/w_0))^2$$

The drawback of this technique is that diagnosing test is expensive for this method. The clavicle detection detection system suppress false positive rates. The AUC value is 84.12%. The overall accuracy is low compared to the previous technique. Hence this major point leads to a drawback of this technique. Technique [9] uses the patient siobnodfe condit the graph segmentation framework. It was published in the IEEE 10th symposium on Biomedical Imaging in 2013. The chest films contain important information about, their interpretation is not trivial which encourage the researchers to develop computer algorithms to assist the radiologist in diagnosis process. Automatic segmentation of anatomical fields is one of the first step of such computer-aided systems. Some of the abnormalities and diagnostic information can be directly extracted from the anatomical boundaries such as total lung capacity which aids in detection of pneumonia, pulmonary atelectasis or obstructive airways disease. The labeling system involves they energy formulation with parameter which regularizes the smoothness degree of solution. Choosing a suitable is important to obtain a better segmentation. The

technique can produce a result of 87%. But, there is a disadvantage that regularization parameter estimation through a classification framework was attempt existing. Technique [10] uses automatic TB screening of chest radiographs. It was published in the IEEE; National Library of Medicine in 2013. The implemented methods are lung segmentation, feature computation, and classification. First, our system segments the lung of the input CXR using a graph cut optimization method in combination with a lung model. For the segmented lung field, our system then computes a set of features as input to a pre-trained binary classifier.

Finally, using decision rules and thresholds, the classifier outputs its confidence in classifying input CXR as a TB positive case. The result is that it combines anxiety data with lung models derived from the training set. We also analysis with various classifier architectures. To increase the performance of lung segmentation, produce ordinary performance related to other schemes. These comparison results test our schemes in the field under real status. The factor sets and most of the classifier planning we tested, provide a identical performance. The accuracy of the system is 89.3%. The drawback of this technique is that portable x-rays set not applicable to process with this method.



Fig.3 Example of abnormal CXR's

The CXR obtained were not clear. Hence there is an inaccuracy in identifying TB. The KNN used here coincides with the normal lung segment edges; hence we have to use other classifiers with more advantage. Hence a classifier with more advantage is used to improve the accuracy of the lung image.

3. DATA

For my experiment, I have used three CXR sets. For the first two sets we train and test our classifiers, and on the third set we train our lung models. The images used for my first set were provided by SKS hospital, Salem and the dataset obtained is from my own relative. I have collected it by putting an effort on this project. For the collected data set, I have performed ground truth lung segmentation. CXR shows an abnormal result; (i.e) left lung field has a cancer nodule.

Our first set is collected by my own effort, is a representative of CXR and it is the dataset of a relative, collected especially for my project. From the dataset, I have

observed the abnormal image and the image is in 12 bit grey levels. For this report, I have calculated the ground-truth radiology confirmed by clinical tests, patient history etc.

Our second CXR set, is provided by the GANGA hospital. It is located in Namakkal. I have collected from my relative who has been suffered from coughing and sneezing for many years and hence I have collected the pus samples and observed it in a clinical centre. It has been tested for TB in the clinical centre. From that report, I have identified that the CXR has an abnormal result. i.e. It has been affected by TB.

Now we train our lung models on a third set from the DHARANYA data set. The data was collected from particularly a medical center in kovai and comprises 20 CXRs. All CXR images have a size of 2048 2048 pixels and a gray- scale color depth of 12 bits. Among the 20 CXRs, 12 CXRs are normal and 8 CXRs are abnormal. Each of the abnormal CXRs contains one pulmonary nodule. However, in the GANGA image set, the nodules hardly affect the lung shapes. The nodules are either well within the lung boundary or they are so subtle that the effects on lung shape are minor. We can therefore take advantage of the entire GANGA database to train our shape model for a typical normal lung. To do so, we use the segmentation masks. For example, Fig. 4 shows an abnormal CXR from the GANGA database together with the outline of the left and the right lung. Note that the left mid lung field in Fig. 4 contains a cancer nodule.

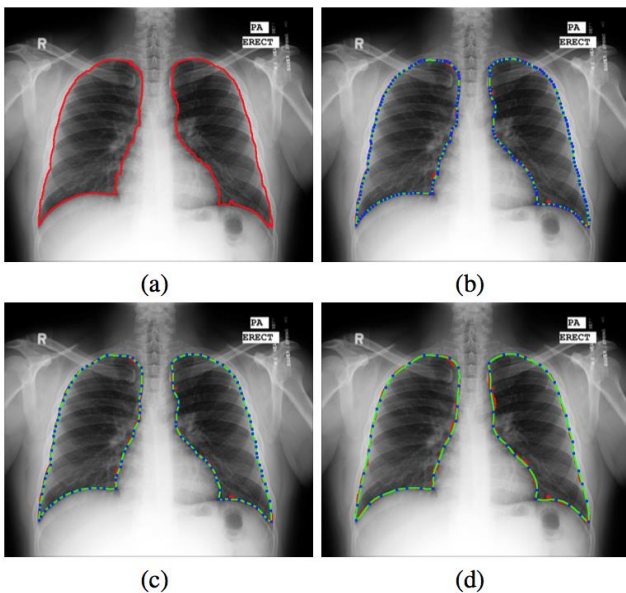


Fig.4 GANGA CXRs with manual ground-truth lung segmentation.

4. METHODS

The methods used in this paper are: lung segmentation, feature computation, and classification. Fig. 5 shows the architecture of our system with the different processing steps, which the following sections will discuss in more detail. First, our system segments the lung of the input

CXR using a graph cut optimization method in combination with a lung model. For the segmented lung field, our system then computes a set of features as input to a Multi-class SVM classifier. Finally, using decision rules and thresholds, the classifier outputs its confidence in classifying the input CXR as a TB positive case.

4.1 GRAPH CUT BASED LUNG SEGMENTATION

Lung segmentation is done from the training masks we have collected. Normally segmentation of medical images has a poor contrast because of the hardware constraints and anatomical shape variations.

Step 1: Align the training masks linearly to a given input CXR.

Step 2: Compute the Histogram representation for the lung model.

Step 3: Note the CXR and its calculated lung model.

Now proceed to the next step, we employ a graph cut model and lung boundary detection with an objective function. Three requirements have to satisfy for this condition.

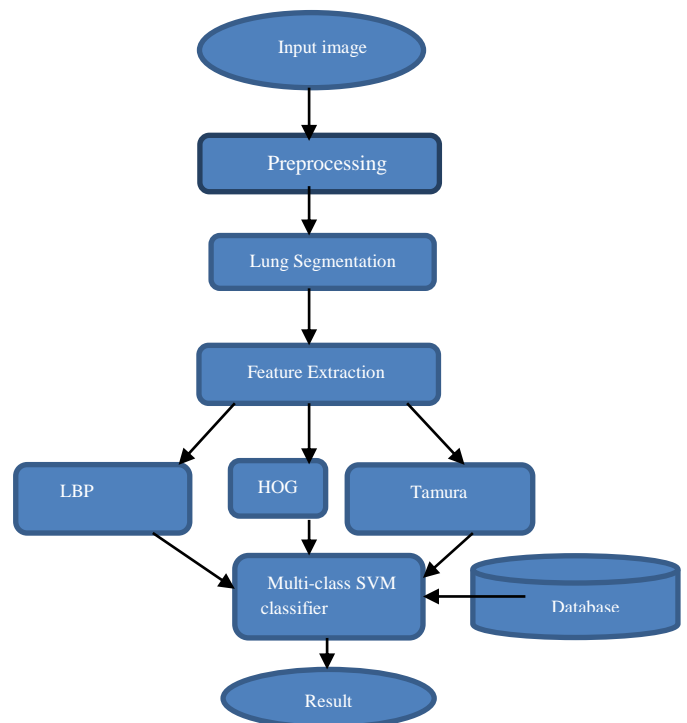


Fig.5 System Architecture.

Image segmentation has come a long way. Using just a few simple grouping cues, one can now produce rather impressive segmentation on a large set of images. Behind this development, a major converging point is the use of the graph based technique. Graph cut provides a clean, flexible, formulation for image segmentation. It provides a convenient

language to encode simple local segmentation cues, and a set of powerful computational mechanisms to extract global segmentation from the simple local/pairwise pixel similarity. Computationally graph cuts can be very efficient.

1. Minimum cuts and maximum flow
2. Human image segmentation
3. Grouping intensities and texture
4. Multi-scale graph cut

A graph cut is a partition of the vertices of a graph in to two disjoint subsets. Any cut determines a cut set, the set of edges that have one end point in each subset of the partition. In a connected graph, each cut-set determines a unique cut, and in some cases cuts are identified with their vertex partitions. In the field of computer vision, graph cut is employed specifically to solve a wide variety of low-level computer vision problems. Such energy minimization problems can be reduced in to instances of the maximum flow problems in a graph. Under most formulations of such formulations in computer vision, the minimum energy solution corresponds to a maximum posterior estimate of a solution. De noising a binary image can be solved exactly using this approach. Solutions produced are usually near the global optimum. The general graph-cut for a 1D image is given below. It shows the general graph-cut of a 1D image.

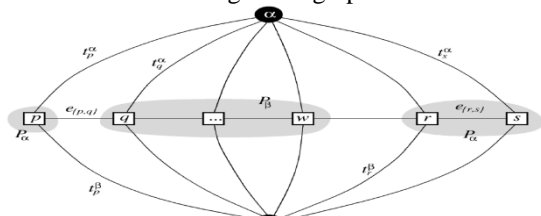


Fig.6 Graph cut for a 1D image

The algorithm of a graph cut model in computer vision label the problems such as segmentation and disparity estimation as energy minimization using an undirected weighted graph $G=(V,E)$. The set of vertices v represents the pixel properties such as intensity; and a set of edges E connects this vertices. The edge weighted graph typically represents the space between the vertices.

4.2 FEATURES

To describe the lung as normal and abnormal (TB affected) experiment should be done using two different feature sets. Our main motivation is to use the features that will match the structures in the chest radiographs.

Object detection features:

The same procedure for earlier TB classification is worked out. First, combination shape, edge and texture descriptors are used. We compute a histogram that shows the distribution of the different descriptor values across the lung field. Each histogram bin is a feature, and all feature of the descriptor is used. (What we have taken as input to the classifier). From empirical results, it has been noticed that 32 bins for each histogram gives a better result.

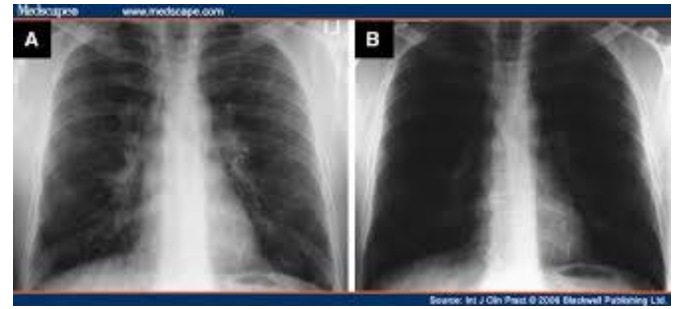


Fig.7 CXR and its calculated lung model

Some shape and texture are:

4.2.1 Intensity Histograms:

Intensity histogram aims at increasing the colour of the image. The grey level image is shown in colour.

4.2.2 Gradient Magnitude Histograms:

It is used to describe the gradients (such as the pixel value). The diagrammatic representation is in fig.8.

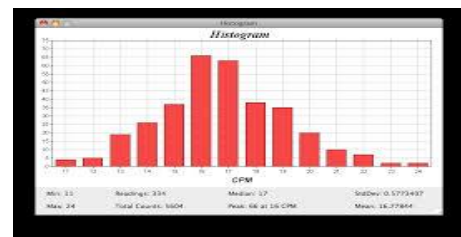


Fig.8 GM Histogram

4.2.3 Shape Descriptor Histogram:

It denotes the shape of the lung image. It can be represented in hessian matrix. It is represented in terms of histogram values.

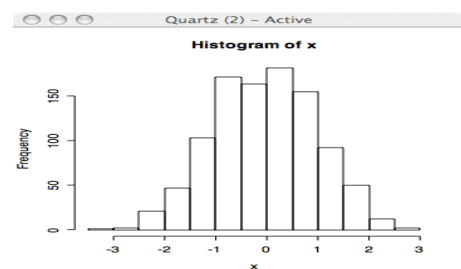


Fig.9 SD histogram

4.2.4 Curvature Descriptor Histogram:

It denotes the angle of the image. The normalisation with respect to intensity makes this descriptor independent of image brightness.

4.2.4.1 HOG

Histogram of oriented gradients are feature descriptors used in computer vision and image processing for the purpose of object detection. This method is similar to that of edge oriented histograms. Scale-invariant feature transform descriptors, and shape contexts, but differs in that it is

computed on a dense grid of uniformly spaced cells and uses overlapping normal contrast normalisation for improved accuracy. HOG is weighted according to gradient magnitude. The image is divided into small computed regions, and for each region a histogram of gradient directions or edge orientations for the pixels within the region is computed. The combination of these histograms represents the descriptor. HOG has been successfully used in many detection systems.

4.2.4.2 LBP

Local Binary Patterns is a type of feature used for classification in computer vision. LBP is the particular case of the "Texture Spectrum Method proposed". LBP was first described, and it has since been found to be a powerful feature for texture classification. It has further been determined that when LBP is combined with the HOG it improves the detection performance considerably on some data sets,

The process of LBP are;

1. Divide the examined window into cells.
2. For each pixel in a cell, compare the pixel to each of its 8 neighbors (on its left top, left middle, left-bottom, right top) etc. Follow the pixels along a circle, i.e. clock-wise or counter-clockwise.
3. Where the centre pixel's value is greater than the neighbour's value, write 1. otherwise write 0. This gives an 8-digit binary number. Because of its computational simplicity and efficiency, it is successfully used in various computer vision applications, often in combination with HOG.

The approach used here is the maximum filter response across all scales. The main application was to enhance blood vessels, which have mostly thin elongated shapes, through filtering. Our main goal is to detect nodular patterns by capturing spherical or elliptical shapes in the local intensity curvature surface.

4.2.5 Content Based Image Features:

The feature collections include intensity, edge, texture, and shape moment features, which are typically used by CBIR systems. We evaluate the effect of high dimensional feature spaces on classification accuracy. We extract most of the features, except the Hu moments and shape features.

4.2.6 Tamura Feature Descriptor:

Today's CBIR systems is used in most cases the set of six visual features, namely,

1. coarseness
2. contrast
3. directionality
4. linelikeness
5. regularity
6. roughness due to distances of notable spatial variations of grey levels, that is, simplicity, to the size of primitive elements (texels) forming the texture.
7. degree of directionality measures the frequency. Distribution oriented local edges against their direction angles.

4.2.6.1 CEDD

Color and Edge Direction Descriptor incorporates the colour and Edge Direction.

4.2.6.2 FCTH

Fuzzy colour and Colour Texture Histogram incorporates the fuzzy colour and Texture of the image. It differs in the way they capture texture information.

4.2.6.3 Hu Moments

These moments are widely used in image analysis. They are invariant under image scaling. They are invariant under image scaling, translation, rotation. We use the distributor, Content-Based Visual Information Retrieval.

4.2.6.4 CLD and EHD

It captures the spatial layout of the dominant colours on an image grid consisting of 8 x 8 blocks represented by DCT.

4.2.6.5 Primitive Length, Edge Frequency and Auto Correlation

This texture analysis method uses statistical rules to describe the spatial distribution and relation of grey values.

4.2.6.6 Shape Features

It uses a collection of shape features provided by the standard MATLAB implementation, such as the area or elliptical shape features of local patterns.

4.3 CLASSIFICATION

We use the Multi-class SVM Classifier for classification. A SVM is a binary classifier, that is, the class labels can only take two values: +1 or -1. Binary Tree Architecture (SVM-BTA) takes advantage of tree architecture and the high classification accuracy of SVM's value. It can also be interpreted as a confidence value, the more confident one is that the point X belongs to the positive class. Enhance the binary classification type of normal and abnormal. In multi-class classification, the types divide into normal stage, beginning stage or severe stage.

4.4 SYSTEM REQUIREMENTS

D-RAM 1-GB is implemented as a hardware to support the process.

MATLAB is a high level technical language and it is implemented as software to support our process. It is a useful interacting environment for algorithm development, data visualisation, data analysis, and numerical computation.

Outside, Matlab images may be of three types, i.e. black and white, grey scale and coloured. In Matlab, however there are four types of images. Black and White images are called binary images, containing 1 for white and 0 for black. Grey scale images are called intensity images, containing numbers in the range of 0 to 255 or 0 to 1. coloured image. First image contains all images may be represented as RGB image or Indexed image. It exactly exist of two matrices namely image matrix or map matrix. Each colour in the image is given an indexed number and its image matrix, each colour is represented as an indexed number.

5. RESULTS

In this section, we perform the TB detection by machine performance, human performance and then finally compare the machine performance with human performance.

5.1 SEGMENTATION OF THE LUNGS USING GRAPH-CUT

We should observe the CXRs obtained from different patients and different clinics and then we should perform the graph-cut segmentation. From this segmentation, we observed some of the CXRs as normal (they are in regular lung shape) and some of the images are abnormal (TB affected).

First we should perform the segmentation and then we should classify the images using three different classifiers.



Fig.10 Graph-cut segmentation image.

5.2 CLASSIFIER PERFORMANCE

We should compare the CXRs with three different classifier.

5.2.1 SKS Hospital:

One of the CXRs obtained is abnormal and its accuracy is first noted using the KNN classifier. It got an accuracy of about 75.3%. By performing classification using the SVM classifier, an accuracy of about 89.9% is obtained. The same CXR is performed classification using the Multi-class SVM classifier. We achieve an accuracy of about 94.3%.

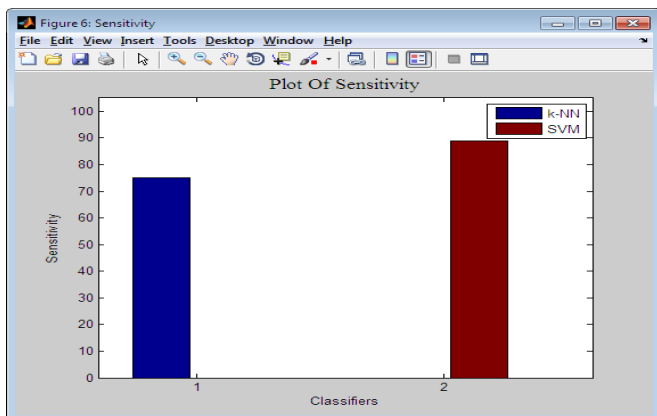


Fig 11. Comparison of classification between KNN and SVM classifiers.

5.2.2 Ganga Hospital:

We should perform the experiment as we done in the SKS Hospital set. Using kNN classifier, we measured an accuracy of about 70.9% and using Multi-class SVM classifier we achieved a accuracy of about 76.9% and using Multi-class SVM classifier we achieve an accuracy of about 84.5%.

5.2.3 Dharanya Clinic:

We should perform the same experiment as we done in the GANGA Hospital set. First, using kNN classifier, we measure an accuracy of about 83.4%. Using SVM classifier, we measure an accuracy of about 86.5% and using Multi-class SVM classifier. We measure an accuracy of about 92.6%.

Finally we should compare the classification of three classifiers.

TABLE I: Comparison table of kNN,SVM&Multi-class SVM classifier.

CLASSIFIER	SKS Hospital	GANGA Hospital	DHARANYA Clinic
kNN	75.3%	70.8%	83.4%
SVM	89.9%	76.9%	86.5%
Multi-class SVM	94.3%	84.5%	92.6%

5.3 COMPARISON WITH OTHER CLASSIFIERS

The other classifiers, used in our previous experiments, measured an accuracy below our observed results. (i.e.) from 70% and below 70%. Hence our classifiers are the best in measuring the accuracy of TB. From the results of three hospital, the classifiers we used measures a better accuracy. Hence they are better in identifying TB with more accuracy. But our main motive is to find the classifier with best accuracy. By comparing the accuracy of three classifier, we can obtain the result.

5.4 COMPARISON WITH HUMAN PERFORMANCE

In earlier methods, we have used several methods to measure the accuracy and diagnosing TB. As years passed by, everyone should move in progress in all departments. Especially in the medical field, everyone approaches a new technique for the manifestation of the disease. The advantage in our classifier is, it is suitable for all the people (poor, middle & high-class). It finds a best result in achieving the performance of the human experts.

5.5 COMPARISON OF CLASSIFIER ACCURACY

For this comparison, an approximate of 150 lung images can be used to identify the classifier with best accuracy.

Note: The number of images used here is a approximate value and it doesn't related to our experiment. For our experiment we used few data sets to compare the accuracy.

TABLE II: Comparison of Classifier Accuracy

TECHNIQUE USED	NUMBER OF IMAGES	ACCURACY
k-Nearest Neighbours	150	75% Normal Analysis 78% Abnormal Analysis
Binary-Support Vector machine	150	89% Normal Analysis 87% Abnormal Analysis
Multi-class Support vector machine	150	92% Normal Analysis 90% Abnormal Analysis

6. CONCLUSION

In this paper, we have developed an accurate method for the manifestation of TB. We have used different classifiers and identified which is the best classifier in TB manifestation. By taking CXR as input, we have compared it with different classifiers and measured the accuracy, that is up to the performance of the human experts. From the results, we have identified that Multi-class SVM classifier is the best in detecting TB with more accuracy. Hence this *Multi-class SVM Classifier* is promising in achieving the performance of the human experts.

ACKNOWLEDGEMENT

I would like to thank Dr.P. Muralidharan, DM. MD, Dharanya Clinic, Kovai, for providing me the CXRs set for TB manifestation.

REFERENCE

[1] Y. Boykov, O. Veksler, and R. Zabih, "Fast approximate energy minimization via graph cuts," *IEEE Trans. Pattern Anal. Mach. Intell.*, vol. 23, no. 11, pp. 1222–1239, Nov. 2001.

[2] J. Shiraishi, S. Katsuragawa, J. Ikezoe, T. Matsumoto, T. Kobayashi, K. Komatsu, M. Matsui, H. Fujita, Y. Kodera, and K. Doi, "Development of a digital image database for chest radiographs with and without a lung nodule," *Am. J. Roentgenol.*, vol. 174, no. 1, pp. 71–74, 2000.

[3] J. Burrill, C. Williams, G. Bain, G. Conder, A. Hine, and R. Misra, "Tuberculosis: A radiologic review," *Radiographics*, vol. 27, no. 5, pp. 1255–1273, 2007.

[4] J. Burrill, C. Williams, G. Bain, G. Conder, A. Hine, and R. Misra, "Tuberculosis: A radiologic review," *Radiographics*, vol. 27, no. 5, pp. 1255–1273, 2007.

[5] S. Jaeger, S. Antani, and G. Thoma, "Tuberculosis screening of chest radiographs," in *SPIE Newsroom*, 2011.

[6] S. Candemir, S. Jaeger, K. Palaniappan, S. Antani, and G. Thoma, "Graph-cut based automatic lung boundary detection in chest radiographs," in *Proc. IEEE Healthcare Technol. Conf.: Translat. Eng. Health Med.*, 2012, pp. 31–34.

[7] L. Hogeweg, C.I. Sánchez, P.A. de Jong, P. Maduskar, and B. van Ginneken, "Clavicle

segmentation in chest radiographs," *Med. Image Anal.*, vol. 16, no. 8, pp. 1490–1502, 2012.

[8] S. Jaeger, A. Karargyris, S. Antani, and G. Thoma, "Detecting tuberculosis in radiographs using combined lung masks," in *Proc. Int. Conf. IEEE Eng. Med. Biol. Soc.*, 2012, pp. 4978–4981.

[9] S. Candemir, K. Palaniappan, and Y. Akgul, "Multi-class regularization parameter learning for graph cut image segmentation," in *Proc. Int. Symp. Biomed. Imag.*, 2013, pp. 1473–1476.

[10] Automatic Tuberculosis Screening Using Chest Radiographs-Stefan Jaeger*, Alexandros Karargyris, Sema Candemir, Les Folio, Jenifer Siegelman, Fiona Callaghan, Kannappan Palaniappan, Rahul K. Singh, Sameer Antani, George Thoma, Yi-Xiang Wang, Pu-Xuan Lu, and Clement J. McDonald-IEEE transactions on medical imaging, vol. 33, no. 2, February 2014.

[11] MATLAB. ver. 7.4.0.287 (R2007a), Math Works, Natick, MA, 2007.

[12] V. Vapnik, *The Nature of Statistical Learning Theory*. New York: Springer Verlag, 2000.

[13] B. Schölkopf, C. Burges, and A. Smola, *Advances in Kernel Methods: Support Vector Learning*. Cambridge, MA: MIT Press, 1999.

[14] D. Seghers, D. Loeckx, F. Maes, D. Vandermeulen, and P. Suetens, "Minimal shape and intensity cost path segmentation," *IEEE Trans. Med. Imag.*, vol. 26, no. 8, pp. 1115–1129, Aug. 2007.

[15] B. Ginneken, A. Frangi, J. Staal, B. Romeny, and M. Viergever, "Active shape model segmentation with optimal features," *IEEE Trans. Med. Imag.*, vol. 21, no. 8, pp. 924–933, Aug. 2002.

[16] Y. Shi, F. Qi, Z. Xue, L. Chen, K. Ito, H. Matsuo, and D. Shen, "Segmenting lung fields in serial chest radiographs using both population based and patient-specific shape statistics," *IEEE Trans. Med. Imag.*, vol. 27, no. 4, pp. 481–494, Apr. 2008.

[17] S. Candemir, S. Jaeger, K. Palaniappan, J. Musco, R. Singh, Z. Xue, A. Karargyris, S. Antani, G. Thoma, and C. McDonald, "Lung segmentation in chest radiographs using anatomical atlases with non-rigid registration," *IEEE Trans. Med. Imag.*, to be published.

[18] A. Hoog, H. Meme, H. van Deutekom, A. Mithika, C. Olunga, F. Onyino, and M. Borgdorff, "High sensitivity of chest radiograph reading by clinical officers in a tuberculosis prevalence survey," *Int. J. Tuberculosis Lung Disease*, vol. 15, no. 10, pp. 1308–1314, 2011.

[19] P. Maduskar, L. Hogeweg, H. Ayles, and B. van Ginneken, "Performance evaluation of automatic chest radiograph reading for detection of tuberculosis (TB): A comparative study with clinical officers and certified readers on TB suspects in sub-Saharan Africa," in *Eur. Congr. Radiol*, 2013.

[20] D. Beard, "Firefly—Web-based interactive tool for the visualization and validation of image processing algorithms," M.S. thesis, Univ. Missouri, Columbia, 2009.